Materials Science & Engineering C 123 (2021) 111960

Contents lists available at ScienceDirect

Materials Science & Engineering C

journal homepage: www.elsevier.com/locate/msec

Saccorhiza polyschides used to synthesize gold and silver nanoparticles with enhanced antiproliferative and immunostimulant activity

N. González-Ballesteros [a,1], L. Diego-González [b,c,1], M. Lastra-Valdor [d], M. Grimaldi [e], A. Cavazza [e], F. Bigi [e,f], M.C. Rodríguez-Argüelles [a,*], R. Simón-Vázquez [b,c,**]

[a] Departamento de Química Inorgánica. CINBIO. Universidade de Vigo, 36310 Vigo, Spain
[b] Immunology Group. CINBIO, Universidade de Vigo, 36310 Vigo, Spain
[c] Instituto de Investigación Sanitaria Galicia Sur, Hospital Álvaro Cunqueiro, 36312 Vigo, Spain
[d] Centro de Investigación Marina, Universidade de Vigo, 36331 Vigo, Spain
[e] Dipartimento Scienze Chimiche, della Vita e della Sostenibilità Ambientale, Università di Parma, 43124 Parma, Italy
[f] IMEM Parma-CNR, 43124 Parma, Italy

ARTICLE INFO

Keywords:
Green synthesis
Saccorhiza polyschides
AuNP
AgNP
Cancer
Antiproliferative activity
Immunotherapy
ROS

ABSTRACT

Over the last years, there has been an increasing trend towards the use of environmentally friendly processes to synthesize nanomaterials. In the case of nanomedicine, the use of bionanofactories with associated biological properties, such as seaweed, has emerged as a promising field of work due to the possibility they open for both the preservation of those properties in the nanomaterials synthesized and/or the reduction of their toxicity. In the present study, gold (Au@SP) and silver (Ag@SP) nanoparticles were synthesized using an aqueous extract of *Saccorhiza polyschides* (SP). Several techniques showed that the nanoparticles formed were spherical and stable, with mean diameters of 14 ± 2 nm for Au@SP and 15 ± 3 nm for Ag@SP. The composition of the biomolecules in the extract and the nanoparticles were also analyzed. The analyses performed indicate that the extract acts as a protective medium, with the particles embedded in it preventing aggregation and coalescence. Au@SP and Ag@SP showed superior immunostimulant and antiproliferative activity on immune and tumor cells, respectively, to that of the SP extract. Moreover, the nanoparticles were able to modulate the release of reactive oxygen species depending on the concentration. Hence, both nanoparticles have a significant therapeutic potential for the treatment of cancer or in immunostimulant therapy.

1. Introduction

In recent decades, the use of nanomaterials, especially metal nanoparticles, has attracted considerable attention due to their electronic and chemical properties, as well as their application in a large number of fields, including nanomedicine [1]. Some examples that illustrate their numerous applications are the antimicrobial activity of silver nanoparticles (AgNPs) [2,3] or the use of gold nanoparticles (AuNPs) in imaging, therapy and nanotheragnosis [4–8].

The development of nanomaterials is closely related to the study of new methods of synthesis. Among them, the so-called green methods, which enable the production of nanomaterials in an eco-friendly and cost-effective manner, occupy a prominent place. Besides, nanomaterials synthesized using green methods can preserve and even improve the therapeutic properties provided by the organisms employed in their synthesis, such as plants, bacteria or algae [9–16]. These organisms possess natural compounds, such as polysaccharides, polyphenols, pigments or proteins, with relevant antioxidant, anti-inflammatory or antibacterial activity, among other biological properties.

In recent years we have been working with seaweed to obtain different AuNPs and AgNPs with the aim of evaluating their antitumor or immunostimulant activity [17–19].

For the present work, the brown macroalga *Saccorhiza polyschides* (SP) was selected for the synthesis of gold (Au@SP) and silver (Ag@SP) NPs to test their potential immunostimulant activity. SP is a large kelp-

* Corresponding author.
** Correspondence to: R. Simón-Vázquez, Inmunology Group. CINBIO, Universidade de Vigo, 36310 Vigo, Spain.
E-mail addresses: mcarmen@uvigo.es (M.C. Rodríguez-Argüelles), rosana.simon@uvigo.es (R. Simón-Vázquez).
[1] Co-first authors.

https://doi.org/10.1016/j.msec.2021.111960
Received 30 September 2020; Received in revised form 2 February 2021; Accepted 8 February 2021
Available online 12 February 2021

like macroalgae, with an abundant presence in the lower littoral zone of the North East Atlantic coast, where it colonizes hard substrata in the sublittoral. SP is an annual species with an extremely fast growth rate during spring and summer, which accounts for its high bioavailability. Currently, it is mainly used as a source of alginic acid [20]. However, extracts of SP have recently been studied due to their hypoglycemic, antiplasmodial, antiinflamatory and cytotoxic features [21–23].

Some of the biological activities of brown seaweed are due to the presence of fucoidans, which are sulphated polysaccharides abundant in this type of seaweed that have been claimed to have antitumor and immunostimulant properties, among other biological effects [24–28]. For instance, it has been demonstrated that fucoidans can interact with cells of the immune system, such as natural killer cells (NK) or dendritic cells (DCs), and promote an innate or adaptive immune response against tumor cells [29,30]. These cells usually create an immunosuppressive environment in the tumor microenvironment to evade immune response [31–33]. The reactivation of the immune system can help to detect tumor cells and eliminate them. Moreover, the combination with chemotherapy increases the efficiency of immunotherapy and the possibility to eradicate the cancer [34,35].

The activation of the immune system against tumor cells is induced by the recognition of aberrant proteins or molecules by innate immune cells, mainly DCs [36]. These cells can internalize and process those molecules and present some antigenic peptides, through specific receptors on the surface (the major histocompatibility complex, MHC), to the naïve T cells that will produce an adaptive immune response against the antigen that is present in the aberrant molecule. Depending on the stimulus, these naïve T helper (Th) cells can be differentiated into Th1 cells, which will promote a cellular immune response mediated by cytotoxic T lymphocytes (Tc), or Th2 cells, which will interact with B lymphocytes and promote a humoral response based on the production of specific antibodies [37]. Finally, the Tc and antibodies will recognize those antigenic molecules on the surface of the tumor cells and kill them or attract other effector cells to destroy them. In a cancer therapeutic vaccine, a Th1 immune response is usually more efficient and the use of adjuvants that promote this type of immune response is desirable [36,38]. For that reason, the search for new and biocompatible adjuvants and the use of nanomaterials as antigen and adjuvant carriers is an area of growing interest [39].

Apart from fucoidans, other seaweed components, such as phenolic compounds, have also shown interesting biological properties, *e.g.* antitumor and antioxidant activity [40,41].

In this study, the effect on cell viability of SP aqueous extract and the NPs synthesized was tested on a human pulmonary epithelial and a promyelocytic cell line. Also, the potential activation of some proteins and cells of the immune system and the capacity to stimulate a Th1 immune response was explored for the SP extract, Au@SP and Ag@SP *in vitro* to characterize the potential immunostimulant effect that, in combination with the antiproliferative activity, could be useful in an antitumor therapy.

2. Experimental section or materials and methodology

2.1. Preparation and characterization of SP extract, Au@SP and Ag@SP

The protocols used for the preparation of SP extract, Au@SP and Ag@SP are based on the ones we have previously reported for other macroalgae with some modifications [17–19]. All this information is shown in detail in the Supplementary Section, along with the characterization techniques employed.

2.2. In vitro antioxidant activity

The reducing power, total phenolic content (TPC) and the 2,2 Diphenyl 1 picrylhydrazyl (DPPH) radical scavenging activity of SP extract, Au@SP and Ag@SP were measured employing our methods, previously described [19,42].

2.3. Cell lines

The human cell lines A549 (lung epithelial cells) and HL-60 (promyeloblast cells) were provided by the American Type Culture Collection (ATCC). The culture medium was RPMI 1640 supplemented with 10% of fetal bovine serum and 2% of antibiotic (penicillin/streptomycin).

2.4. Cell viability assay

Cell viability was determined by an impedance-based assay using the xCelligence Real Time Cell Analysis Instrument (Acea Biosciences, Inc.). Changes in cell viability were measured in real time for the A549 cell line by recording variations in the impedance (cell index) induced by cell attachment or detachment.

A549 cells were seeded at a density of 1×10^4 cells/well on a xCelligence plate and allowed to attach and rest for 24 h before the samples were added. The *SP* extract, Au@SP and Ag@SP were tested at 100 mg/mL, 40 μM [Au] and 16 μM [Ag], respectively. Moreover, four serial dilutions of each sample were also added in order to calculate the IC50. After the addition of the samples, the cells were incubated for another 48 h. Cells in culture medium alone were used as reference. Moreover, to discard any interference of the treatments with the method, samples in culture medium and culture medium alone were also monitored. The cell index was normalized to the untreated cells.

2.5. Reactive oxygen species (ROS) release

ROS production induced by the treatments was determined on HL-60 cells as described before [18]. The concentrations tested were 100 and 2 mg/mL for SP extract, 40 and 1 μM [Au] for the Au@SP, 16 and 1 μM [Ag] for the Ag@SP.

2.6. Cytokine release

The potential release of cytokines from immune cells incubated with SP extract, Au@SP and Ag@SP was tested on human peripheral blood mononuclear human cells (hPBMCs), as already described [18]. The cytokines measured were granulocyte-macrophage colony–stimulating factor (GM-CSF), interferon gamma (INF-γ), interleukin 10 (IL-10), interleukin 6 (IL-6) and tumor necrosis factor (TNF-α).

2.7. Statistical analysis

A Shapiro-Wilk test was conducted to determine the normal distribution of the samples. Depending on the normality and the number of samples, a one-way analysis of variance (either an ANOVA or a Kruskal-Wallis test), followed by a Tukey's or Dunn's test or a comparison between two means (T-student or a Mann Whitney test), was conducted to ascertain significant differences using GraphPad Prism 8 software. Each experiment was performed at least three times ($n \geq 3$) and the results were represented as mean ± standard deviation (SD). In the graphs, results are indicated as: no significant (ns) $P > 0.05$, * $P \leq 0.05$, ** $P \leq 0.01$, *** $P \leq 0.001$, **** $P \leq 0.0001$.

3. Results and discussion

3.1. Synthesis and UV–visible characterization of gold and silver nanoparticles

SP extract was used in the reduction of Au(III) and Ag(I) to Au(0) and Ag(0), respectively. To achieve a narrow size distribution, the optimal reaction conditions were established after several trials using different experimental conditions each time, modifying parameters such as

seaweed extract concentration, metal concentration, temperature, and time.

Regarding the synthesis of Au@SP, a change in color, from pale yellow to red, was observed after 24 h of reaction at room temperature. UV–Vis spectra analysis (Fig. 1A) showed the presence of the Surface Plasmon Resonance (SPR) band with λ_{max} at 534 nm. When using higher concentrations of $HAuCl_4$, the NPs aggregated and precipitated.

In order to thoroughly analyze the reaction process, absorbance measurements at the maximum of absorbance wavelength were recorded every 10 s. Changes in the λ_{max} absorbance *vs.* time are represented in Fig. 1B. The reaction might be divided into three stages. The first stage, between 0 and 30 min, corresponds to the activation process. Next, an increase in absorbance appeared between 0.5 and 2 h, which corresponds to the change in color observed and the time when the nucleation process might take place. After that, it could be observed that the reaction slowed down, but the stabilizing process did not occur. The measurements were stopped after 8 h.

Regarding the synthesis of Ag@SP, different assays at room temperature were performed, but color change or UV–Vis spectroscopic bands were not observed even after 3 days of reaction. When heating, a change in color was observed after 30 min and a narrow SPR band was observed in the UV–Vis analysis. A good size distribution was obtained, as evidenced by TEM characterization. In Fig. 1A, the UV–Vis spectrum of Ag@SP shows the characteristic SPR band with λ_{max} at 413 nm. To the best of our knowledge, the synthesis of AuNPs and AgNPs with *S. polyschides* and other species of the genus *Saccorhiza* has not been reported before.

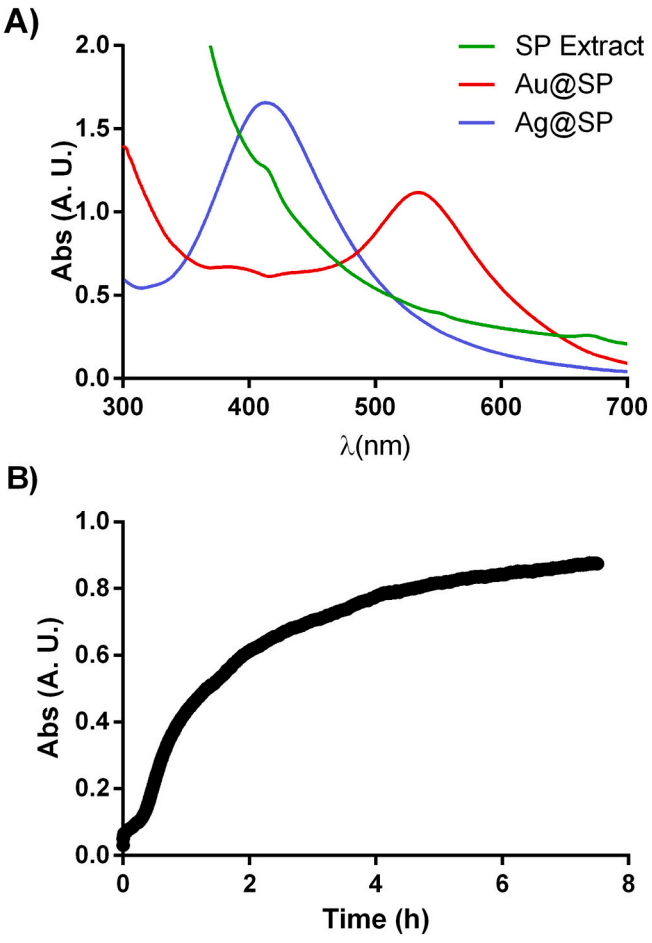

Fig. 1. A) UV–Vis spectra of SP extract Au@SP and Ag@SP showing the SPR bands. B) Time course spectrum measurements of Au@SP showing the changes in the absorbance at 534 nm during the reaction.

The Z potential measurement gives information regarding the surface charge of a colloidal suspension and the stability of the NPs [43,44]. The values obtained for Au@SP and Ag@SP were −10.78 ± 0.74 and −21.88 ± 3.36 mV, respectively, showing the formation of colloidal suspensions of NPs with a negative electrostatic surface charge. Regarding stability, there are guidelines classifying NP-dispersions with Z Potential values of ±0–10 mV, ±10–20 mV, ±20–30 mV and ˃±30 mV as highly unstable, relatively stable, moderately stable, and highly stable, respectively [45]. In this sense, it can be noted that Au@SP possesses lower stability than Ag@SP. Nevertheless, both samples presented good long-term stability (>3 months) when they were preserved at 4 °C.

3.2. Electron microscopy characterization

Transmission electron microscopy (TEM) images were acquired to characterize the size and shape of the NPs obtained. Both Au@SP and Ag@SP appear to be spherical (Fig. 2A and B). The size distribution histograms were calculated, and the average particle sizes obtained were of 13.8 ± 2.3 nm for Au@SP and 15.2 ± 3.2 nm for Ag@SP.

High resolution TEM (HRTEM) was also performed. Fig. 2C and E shows some HRTEM images of the NPs in the extract, along with the corresponding Fourier transform analysis. However, it can be clearly observed that most of the NPs display internal complex contrast. The Fourier transform confirmed that almost all the NPs studied were polycrystalline, which appears to be a general tendency for biosynthesized NPs.

The d-spacing of the crystalline structure of the selected NPs was calculated in the marked area (Fig. 2D and F). The corresponding Miller indices were assigned in accordance with tabulated data. In the case of Au@SP, d-spacings of 0.23 nm and 0.20 nm were measured, which correspond to Miller indices (111) and (002), respectively. In the case of Ag@SP, the preferential d-spacing calculated was 0.20 nm, which corresponds to Miller index (020). The results obtained are in agreement with a face-centred cubic crystalline structure for gold and silver.

In both cases, most of the metallic nanoparticles were embedded in the SP extract matrix. This can be seen in the Dark Field Scanning transmission electron microscopy (DF-STEM) image (Fig. S1). Owing to the Z-contrast mechanism of the high angle annular dark field images (HAADF), NPs showed a brighter contrast than the SP extract.

An Energy Dispersive X-ray Analysis (EDX) was performed (Fig. S2). Apart from gold and silver in the corresponding samples, the presence of other elements in the seaweed was also confirmed. The elements detected in Au@SP samples were C, Ca, Cl, K and O. In Ag@SP samples, Ca and K were not detected, although a signal for iodine was obtained. These results are in accordance with other studies related to the composition of *S. polyschides* [46]. The copper signal that appears in all spectra can be due to the copper grids and to the composition of the seaweed. In fact, several studies have stated that copper is found in this brown seaweed as a trace element [46–48].

From the EDX spectra, the elemental maps of the samples were obtained by selecting carbon and the corresponding metal, gold or silver. The images obtained are shown in Fig. S1. In all cases, the elemental mapping confirmed that C surrounded the metal NPs, while gold and silver were concentrated in the NPs and not within the extract, which confirmed the full reduction of the metal.

In the electron energy loss spectroscopy (EELS) spectra (Fig. S2), the characteristic edge of C (284 KeV), N (401 KeV) and O (532 KeV) was observed. These results confirm the organic nature of the mass surrounding the NPs. Hence, the NPs are embedded in the seaweed extract, which acts, apparently, as a protective agent that keeps the particles apart from one another, preventing their aggregation and coalescence.

3.3. Carbohydrates analysis

Carbohydrates represent one of the main components of seaweed and are constituted by water-soluble sugars and insoluble polymers

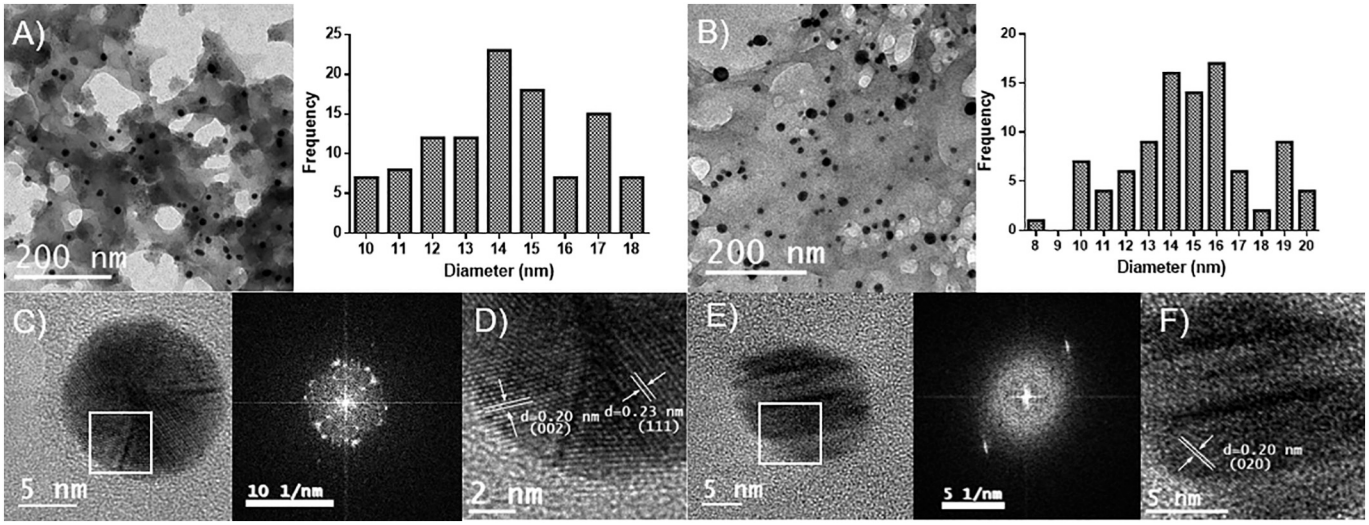

Fig. 2. TEM images of A) Au@SP and B) Ag@SP with their corresponding size distribution histograms. HRTEM images and Fourier transform of C) Au@SP and E) Ag@SP. D) and F). Amplification of the marked area of C and E showing the d-spacing and Miller index calculated.

belonging to fibers. Data reported in the literature concerning carbohydrate analysis in SP seaweed water extracts are often limited to evaluations performed by spectrophotometric assays or indirect measurements and provide scarce information about composition and dimension. The amount of total sugar found is quite variable and has been reported to be, per 100 g of dry weight, about 6.3 g [49], or 16 g [50], or even 45.6 g [46]. In general, all values are lower than those found in other algae species examined.

As for fibers evaluation, an amount of 16.6 g/100 g was determined by García et al., which is a higher value than the mean values obtained for other species analyzed by the same authors [49]. According to Macler, the amount of fibers and soluble sugars is also variable when considering the same species grown in different areas, since algae metabolism is dependent on the availability of nitrogen in seawater [51]. In particular, an inverse relationship between water nitrogen content and fiber amount in algae has been reported by Gómez-Ordóñez et al. [52].

As regards the composition of the carbohydrate fraction, Rodrigues et al. determined, by FTIR-ATR, the presence of alginate, a copolymer of guluronic and mannuronic acids (also confirmed by Pereira et al. [53]), and fucoidans [46].

HPLC-MS analysis performed by Sanchez-Machado et al. also identified the presence of mannuronic and guluronic acids. They calculated a total amount of dietary fibers of 52 g/100 g dry weight [54] (in the range previously reported by Lee et al. [55]).

To our knowledge, no information about molecule dimension and distribution of molecular weight is available for SP algae. Our analysis, performed by steric exclusion chromatography, allowed the separation of several fractions giving a chromatographic profile which is significantly different from those obtained in our previous studies with other algae species [18]. Fig. 3 shows the elution of seven groups of analytes with different molecular weights, which can be attributed to oligo and polysaccharides characterized by different chain lengths. The vertical lines in the figure indicate the retention time of the standard dextrans, which have a known molecular mass and thus permit the attribution of the mass ranges of the analytes generating the different peaks.

The blue line corresponds to the SP extracts and shows that the most abundant fraction (about 60% of the total analytes) is represented by a first large band (named A) with a little tail attached to it (B), both related to the heaviest molecules, characterized by a molecular mass higher than 150 KDa. Then, about 9% is constituted by molecules in the range of 150–50 KDa that could be divided in two distinct bands (peaks C and

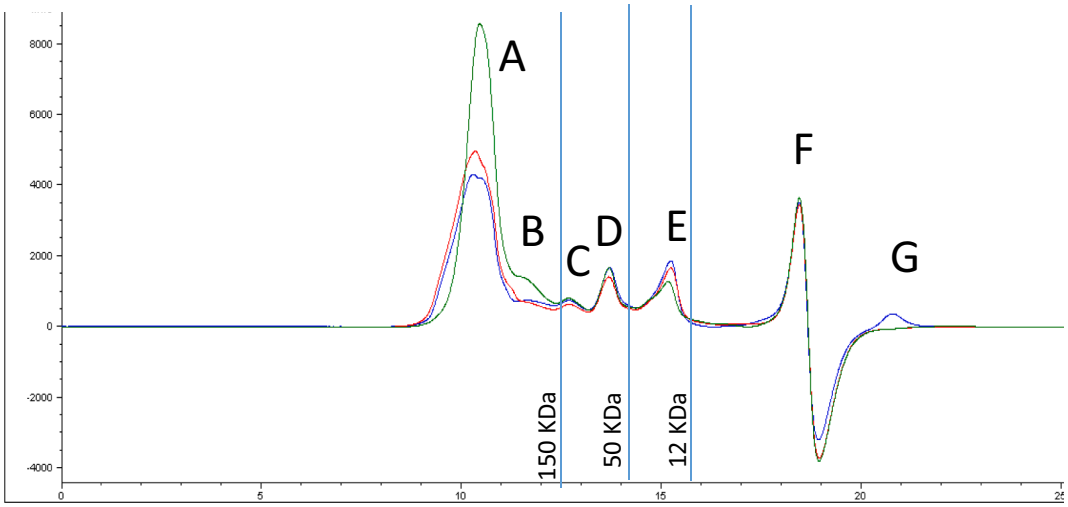

Fig. 3. Carbohydrate profiles of SP extract as such (blue line), and after the formation of Au@SP and Ag@SP (red and green lines, respectively). (For interpretation of the references to color in this figure legend, the reader is referred to the web version of this article.)

D). Band (E), representing carbohydrates with a mass between 50 and 12 KDa, accounts for about 11% of the total analytes. Finally, in the last part of the chromatogram, a small fraction of about 20% is represented by two more bands named F and G, corresponding to lighter molecules, with a mass below 12 KDa.

Comparison between the blue line (alga extract) and the red and the green lines, which represent the extract after the formation of Au@SP and Ag@SP respectively, evidences some relevant differences from the quantitative point of view. Indeed, by comparing the area values of peaks in the three profiles, changes can be observed in the relative amount of carbohydrate fractions with different length chains and, consequently, with different molecular weights. After both NPs formation, the main difference involves the first part of the chromatogram, with an increase in A fraction, which corresponds to about 60% of the total area of the alga extract, 69% after Au@SP formation, and 74% after Ag@SP formation. Peak B, almost absent from the alga extract appears in a clear way only after Ag@SP formation.

No significant differences can be noted for peak C, while band D was slightly lower after the formation of Au@SP. In addition, a sensible decrease in fraction E can be observed, mainly after Ag@SP formation, when it became about 50% smaller than that recorded in the alga extract.

Besides, the complete disappearance of peak G after the formation of NPs indicates that those small molecules, lighter than 12 kDa, were completely consumed during the reaction. All the changes described can be attributed to reactions occurring during the production of nanoparticles, and can be ascribed to the involvement of carbohydrate chains in their formation and/or stabilization, as already suggested in previous works [17,18,56].

3.4. Fourier transformed infrared analysis

Fourier Transform Infra-Red (FTIR) spectral analysis was conducted to identify the biomolecules present in the seaweed extracts before and after the synthesis of NPs. Bands were assigned on the basis of the information provided by other studies regarding the composition of SP [19,46,57]. Since it has been demonstrated that the extracts possess polysaccharides that are present in the seaweed, fucoidan was selected for a comparative analysis between the FTIR spectra of the extract and that of the commercially available polysaccharide. The spectra obtained and the assignation of the bands are shown in Fig. 4.

The broad band that appeared in all spectra between 3460 and 3408 cm^{-1} and the weaker signal at 2940–2928 cm^{-1} could be assigned to O—H and C—H stretching vibrations, respectively, but also to N—H stretching vibrations. The two broad bands at around 1670–1630 and 1460–1380 cm^{-1} are typically assigned to asymmetrical and symmetrical stretching of the carboxylate groups from amide I and II of proteins [58]. Bands between 1200 and 800 cm^{-1} result from C—C and C—O stretching bonds and glycosidic C-O-C vibrations, common to all polysaccharides. The band that can be observed in the spectrum of fucoidan at 1259 cm^{-1} is associated with asymmetric stretching of the O=S=O ester sulphated, while the intense band at 842 cm^{-1} corresponds to the COS bending vibration of sulphate substituents at axial C4 positions [59]. Finally, the bands at 1100–1022 cm^{-1} could be related to the C-OH vibrations of primary alcohol groups [60].

When comparing the spectrum of fucoidan with the ones obtained for the seaweed extracts, the presence of the bands assigned to the polysaccharide can be confirmed, with some changes in the relative intensity. The appearance of new bands can also be noted. In the seaweed, a shift towards lower wavenumbers in the band at 3460 cm^{-1} is observed. On the other hand, a shift to higher wavenumbers in the band at 1637 cm^{-1} can be noted. However, the more significant differences are observed in the bands at 1259 and 1029 cm^{-1}, with modifications in the intensity and appearance of the profile. These changes could be related to the composition of the aqueous extract, which is expected to be a complex mixture of the soluble components of the algae. Since the aqueous extraction is not selective, other biomolecules present in the macroalgae are also extracted, for example, polyphenols and proteins. Hence, the shifts observed in the extracts could be due to the presence of these molecules in association with fucoidan.

When comparing the SP extract with Au@SP and Ag@SP, a different pattern was observed in the shifts of the bands (Fig. 4). Firstly, the peak of 3400 cm^{-1} shifted to lower wavenumbers in the case of Ag@SP while no change is noted in Au@SP, suggesting an involvement of the hydroxyl functional groups from polyphenols and polysaccharides or the amino groups of proteins in the bioreduction of silver. The peak that corresponds to carbonyl stretching at 1600 cm^{-1} shifted to lower wavenumbers in the case of Au@SP but not change is observed in Ag@SP. This is in agreement with other studies which have suggested that the carbonyl group from proteins has a strong capacity to bind metals and that they might be able to cap AuNPs and to prevent agglomeration [61]. Lastly, the band at 1250 cm^{-1} shifted to higher wavenumbers in the case of Ag@SP and to lower ones for Au@SP, with a significant decrease in intensity, which could indicate that sulfonic

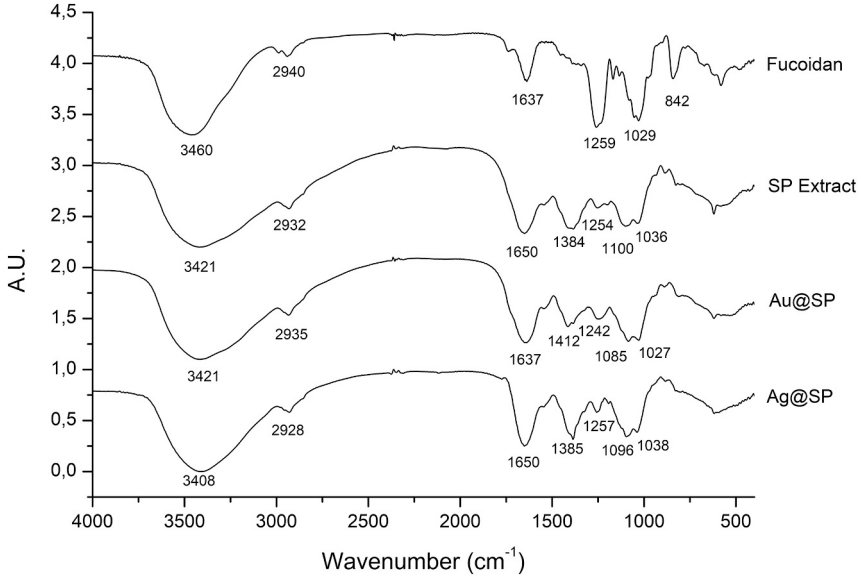

Fig. 4. FTIR spectra obtained for fucoidan, SP extract, Au@SP and Ag@SP.

groups from polysaccharides are involved in metal binding.

3.5. In vitro antioxidant activity

To evaluate the potential use of SP extract as a reducing agent in the synthesis of nanomaterials, the reducing power, TPC, and DPPH scavenging activity were evaluated.

The values obtained for the aqueous extract of SP extract were 67.0 ± 1.2 mg ascorbic acid/g seaweed for the reducing power, 0.41 ± 0.02 mg GAE/g seaweed for the TPC and an EC50 of 76.0 mg/mL for the DPPH scavenging activity. This result confirmed the presence of reductants in the extracts.

To the best of our knowledge, this is the first report on the reducing power of *Saccorhiza polyschides*. Some authors have previously reported on the TPC and DPPH scavenging activity of SP. However, comparison with their results poses certain difficulties since different extraction methods and solvents highly affect the results. Also, the methods used for the determination of the TPC and DPPH scavenging activity also vary, with changes in the reference substance and times of exposition [46,62].

However, we can compare the results obtained in this study with those we obtained for the brown macroalgae *Cystoseira baccata* [19], *Sargassum muticum* [63] and *Desmarestia menziesii*, the red *Palmaria decipiens* [42] and the green seaweed *Ulva lactuca* and *Ulva intestinalis* [11,17]. It has been observed that SP extract possesses a lower reducing power than the brown seaweed *C. baccata*, *D. menziesii* and *S. muticum*, which present values between 9 and 2 times higher, respectively. On the other hand, SP possesses higher reducing power than the red seaweed *P. decipiens* and the green *U. lactuca* and *U. intestinalis*.

When comparing the TPC result, a direct relationship between reducing power and TPC is observed. *C. baccata*, *S. muticum* and *D. menziesii* possess between 6 and 2 times more TPC than SP, while SP possesses higher values than *P. decipiens*, *U. lactuca* and *U. intestinalis*.

Fig. 5 shows the results obtained for SP extract, Au@SP and Ag@SP. A 1.4-fold decrease in the reducing power of Au@SP can be observed, 2.2-fold in the TPC, and 1.4-fold increase in the EC50 value. Regarding Ag@SP, the reducing power increased 1.1 times, the TPC decreased 1.6 times, and the EC50 value decreased 2.0 times.

These results suggest an active role of the phenolic compounds in the reduction of both metals during the synthesis of the NPs. Interestingly, a different behavior is observed regarding the reducing power and DPPH scavenging activity of the extract after the synthesis of Au@SP and Ag@SP. In the first case, a decrease in antioxidant potential is observed in both assays for Au@SP. This could be expected since the biomolecules present in the extract were employed for the reduction of Au(III) to Au (0). In the case of Ag@SP, by contrast, the antioxidant activity of the extract was enhanced. These data are in line with other studies which have shown that the presence of NPs enhances the values obtained, even though the seaweed biomolecules are the ones with the most significant effect on antioxidant activity [64]. Although the mechanism whereby this phenomenon occurs is still unclear, two possible explanations have been proposed. On the one hand, it has been suggested that the antioxidant activity of the NPs is due to the shifting of the electron found in oxygen to the odd electron located at surface orbits of oxygen in •OH and O_2^{-}• radicals [65]. On the other hand, other authors have proposed that the antioxidant activity might be due not only to the presence of capped functional groups, but also to their unique size to volume ratio. Generally, the smaller the particle size, the larger the surface area and, therefore, the higher the number of active sites provided to scavenge the free radicals and inhibit the oxidation reactions [66]. In this case, both Au@SP and Ag@SP present similar diameters, so the difference in their behavior could be related to the fact that silver acts as a good reductant and can lose electrons more easily than gold [56,67].

3.6. Antiproliferative effect of the SP extract, Au@SP and Ag@SP in a human lung epithelial cell line

First, the samples were tested to make sure they were free of any bacterial contamination (Fig. S3) that could interfere in the biological effects observed *in vitro*. The characterization of the potential antiproliferative effect of the samples at different concentrations was evaluated by a cell-impedance assay in real time in the human lung epithelial cell line A549 (Fig. S4). After 48 h of incubation a significant dose-dependent antiproliferative effect was observed in the cells incubated with the SP extract, Au@SP and Ag@SP (Fig. 6). Moreover, morphological changes were observed in the cells by optical microscopy (Fig. S5), namely, the loss of the elongated shape and cell detachment. In addition, preliminary experiments of flow cytometry in A549 cells labelled with Annexin *V*/Propidium iodide (PI) revealed the induction of early apoptosis (Fig. S6).

Ag@SP had the lowest IC50 value (4.0 ± 0.6 μM Ag, 12.5 ± 1.9 mg/mL SP extract) compared to Au@SP (13.2 ± 1.7 μM Au, 33 ± 4.2 mg/mL SP extract) and the SP extract (28.5 ± 1.1 mg/mL). Thus, Ag@SP increased the antiproliferative effect of the SP extract, while Au@SP preserved a similar activity, in agreement with the toxicity of the AgNPs and the general cytocompatibility of AuNPs, respectively, from chemical synthesis [68,69]. In fact, the toxicity of the AuNPs is mainly related to the surface ligands, but not to the NPs themselves [70].

The antiproliferative effect of the SP extract, Au@SP and Ag@SP on tumor cells has already been described for other AuNPs and AgNPs synthesized by green methods. Indeed, previous works with other seaweed showed this effect in colon cancer cell lines [17,19]. Particularly, AuNPs from the brown algae *C. baccata* at 50 μM [Au] induced a decrease of the cell viability of more than 50% on the Caco-2 and HT-29 cell lines after 48 h of incubation [19]. A similar effect was observed on HT-29 cells incubated with AuNPs and AgNPs synthesized from an aqueous extract of the green algae *U. lactuca*, with the highest cytotoxic activity detected at 170 μM [Ag] for AgNps [17]. In both cases, a strong

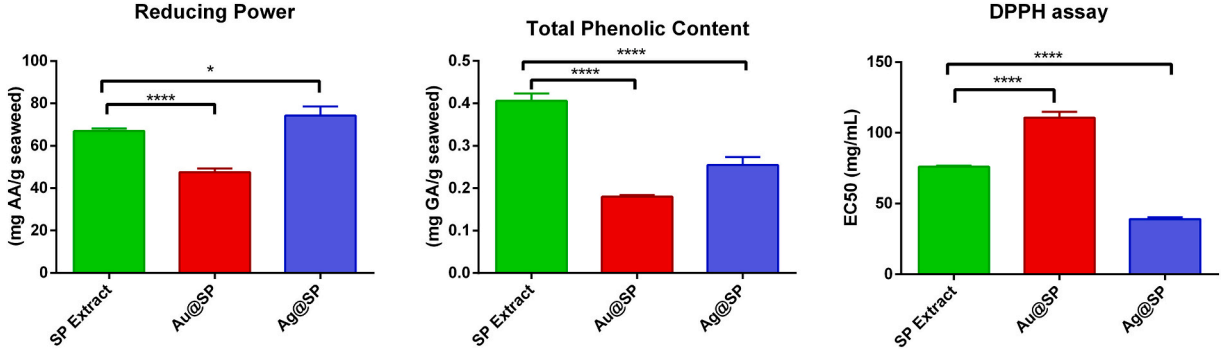

Fig. 5. Reducing activity, TPC, and DPPH scavenging activity of SP extract, Au@SP and Ag@SP. In the graphs: no significant (ns) $P > 0.05$, * $P \leq 0.05$, ** $P \leq 0.01$, *** $P \leq 0.001$, **** $P \leq 0.0001$.

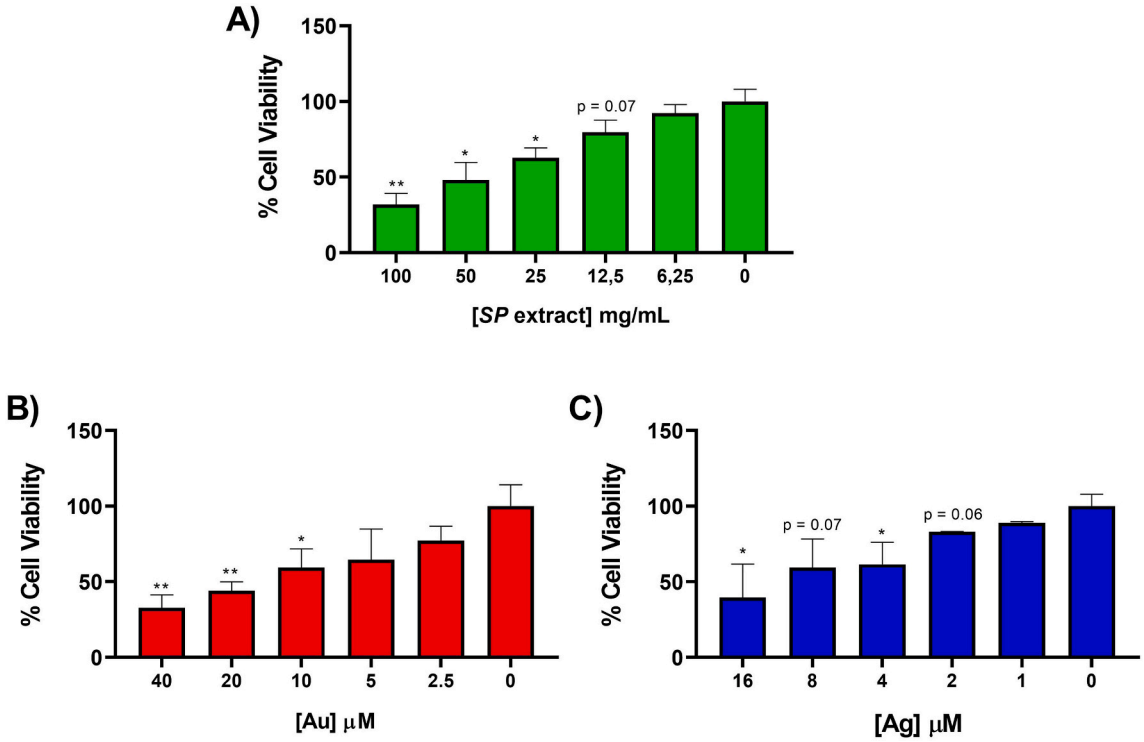

Fig. 6. Percentage of cell viability of A549 cells after 48 h of incubation with (A) SP extract, (B) Au@SP or (C) Ag@SP at different concentrations. In the graphs: * $P \leq 0.05$, ** $P \leq 0.01$.

apoptotic activity was associated to this decrease in cell viability, as detected by an Anexin V-FITC test and the activation of different caspases.

In general, the metal concentration in Ag@SP at the IC50 for A549 cells was much lower than in other AgNPs from natural extracts and the size was also more homogeneous, such as in the case of NPs obtained from *Artemisia princeps* or blushwood berry extract [81,82]. Moreover, Ag@SP were also more efficient than other AgNPs from chemical synthesis [83,84], although the variability among these chemically produced NPs is also high and depends on the method of synthesis and physicochemical characteristics such as size, charge, solubility, or the concentration of free Ag^+ [85,86]. For Ag@SP, the antiproliferative effect is associated not only with the silver core, but also with the extract and, for this reason, the metal concentration is much lower than in those NPs.

In the case of Au@SP, the metal concentration was similar to that in AuNPs from green synthesis, *e.g.* the NPs synthesized from *Marsdenia tenacissima* [87]. Regarding AuNPs from chemical synthesis, as mentioned before, the toxicity is mainly attributed to the different ligands on the surface to stabilize the NPs, but not to the metal [70] and, consequently, the toxicity of Au@SP is due to the SP extract. In fact, the SP extract concentration in Au@SP was similar to the SP extract concentration at the IC50 (Table 1). Hence, the range of therapeutic concentrations of AuNPs and AgNPs from green synthesis can be extremely broad depending on the extract used for the synthesis and the NP's physicochemical properties.

Table 1
IC50 values of the SP extract, Au@SP or Ag@SP in A549 cells after 48 h of incubation.

	[SP] mg/mL	[Au] μM	[Ag] μM
SP Extract	28.5 ± 1.1	n.a.	n.a.
Au@SP	33 ± 4.2	13.2 ± 1.7	n.a.
Ag@SP	12.5 ± 1.9	n.a.	4.0 ± 0.6

n.a.: not applicable.

The antitumor properties of the SP extract, Au@SP and Ag@SP could be associated with the presence of fucoidans and phenolic compounds, as shown in the FTIR analysis (Fig. 4). Fucoidan showed antitumoral activity in different cell lines and in tumor animal models that was highly dependent on the molecular weight, monosaccharide composition and sulphate content, among other properties. These properties, apart from the fucoidan source, are also determined by the method selected for the extraction and purification of this heterogeneous polysaccharide [24]. Phenolic compounds are organic structures based on a common aromatic ring with one or more hydroxyl groups that are difficult to isolate from natural sources [88]. Crude extracts or isolated phenolic acids show a potent antiproliferative activity *in vitro* with different cell lines that seems to be associated with the presence and the number of hydroxyl groups [88]. Both, fucoidans and phenolic compounds, are a complex family of natural compounds that are able to exert their anticancer activity by means of different mechanisms, depending on their structure and composition. For instance, ROS release, cell cycle arrest, modulation of relevant signaling pathways or apoptosis are some of the mechanisms that can be induced by both types of compounds [24,88]. In addition, the contribution of other components of the extract to the antiproliferative activity observed in the A549 cells cannot be discarded.

In summary, we have characterized the antiproliferative effect of the SP extract on a human pulmonary cell line. Besides, Au@SP and Ag@SP preserved those properties and, in the case of Ag@SP, an increase in the toxicity induced by the SP extract was observed, reducing the dose of extract needed for a therapeutic effect.

3.7. ROS release in promyelocytic HL-60 cells

ROS production has usually been associated with cell stress and damage, which could lead to cell death [89]. However, in the last years, some studies have shown that low to moderate ROS production could play an important role in some signaling pathways [90] and in the stimulation of innate immune cells that would help in the development

of a cellular immune response in the presence of a pathogen or an antigen, mediated by Th1 cells [91,92]. In fact, macrophages produce ROS after the detection of foreign molecules as a mechanism of pathogen neutralization [91,93,94]. The human promyelocytic cell line HL-60 was chosen as a model to study ROS production, since these cells are able to modulate this production through a dose-dependent response [95].

Fig. 7 represents the ratio between the median fluorescence intensity (MFI) of the HL-60 cells incubated with the samples for 6 h and labelled with a ROS fluorescent probe and the MFI of the negative control. All the samples induced ROS release at all concentrations tested (Figs. 7 and S7. A). However, ROS levels were only significant at both concentrations (40 and 1 μM) for Au@SP, whereas only the highest concentration of SP extract (100 mg/mL) and Ag@SP (16 μM) induced a significant ROS production. It is noteworthy that in Ag@SP at 16 μM, a 50 mg/mL SP extract concentration is present and, hence, ROS production is not only related to the extract but also to Ag content. Similarly, in 1 μM Au@SP, the SP extract content was 2.5 mg/mL.

The elevated ROS levels at the highest concentration tested for all samples could also induce some toxicity in the HL-60 cells, as seen before for other AuNPs and AgNPs [73,96,97].

In addition, the HL-60 cells were co-treated with the samples and phorbol 12-myristate 13-acetate (PMA), a ROS inductor, to observe the synergistic or antagonistic effect on ROS production (Figs. S7B and S8). The results showed a significant synergistic effect on ROS production at a high concentration, while at a low concentration, a reduction in the ROS levels induced by PMA was observed, possibly due to a potential antioxidant effect. Although a significant inhibition was detected for the SP extract, the NPs were also able to induce a decrease in the ROS level triggered by PMA. This is in accordance with the DPPH scavenging activity (Fig. 5) associated to the phenolic content. Moreover, the differences observed between the extract and the NPs could be due to the different concentration of the phenolic content in the three samples. Additionally, metal nanoparticles synthesized from other extracts, such as plants or microorganisms, have also shown a good capacity to modulate ROS levels and the potential to be used as ROS inductors or antioxidants [98]. In fact, the antimicrobial and antitumoral activity of these NPs is usually associated with ROS release [72,73,98]. Besides the capacity of metals to accept or donate electrons, other factors, such as the method of synthesis, the source of biological material, and the capping agent around the synthetized NPs have a relevant influence on the antioxidant activity.

In summary, Au@SP and Ag@SP could have antibacterial and antitumoral activity due to ROS production at a high concentration, while at a low concentration they could have antioxidant properties, in agreement with the results observed for other NPs synthesized using green methods [14,18]. Besides, they could also induce the activation of different cellular pathways associated with ROS production, as already described.

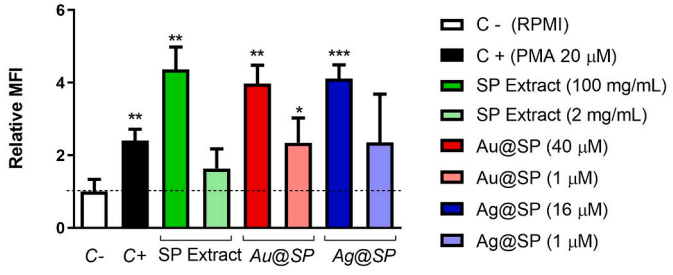

Fig. 7. Increase in the median fluorescence intensity (MFI) of ROS labelled HL-60 cells incubated with the SP extract, Au@SP and Ag@SP at two different concentrations. Cells incubated with PMA at 20 μM were used as positive control. In the graphs: * $P \leq 0.05$, ** $P \leq 0.01$, *** $P \leq 0.001$.

3.8. Cytokines production on hPBMCs incubated with SP extract, Au@SP and Ag@SP

Cytokines are proteins that play a significant role in the communication and activation of the immune system and the inflammation process [99]. For instance, the activation and maturation of the naïve Th cells is mediated, among other factors, by the secretion of cytokines released by the innate and adaptive immune cells [100]. Although cytokine activation is complex and usually implicates several proteins, it has been generally accepted that INF-γ and TNF-α induce Th1 differentiation, while IL-6 and IL-10 are mainly involved in Th2 differentiation [101]. For that reason, the release of these cytokines in hPBMCs incubated with SP extract, Au@SP and Ag@SP was measured. In addition, the production of GM-CSF, a cytokine involved in cell proliferation, was also studied [100]. INF-γ, TNF-α and IL-6 are pro-inflammatory cytokines while IL-10 is mainly regulatory with anti-inflammatory and immunosuppressive properties [101].

A significant cytokine release was observed with all samples tested for IL-6, IL-10 and TNF-α (Fig. 8). However, for GM-CSF the release was only significant with the SP extract and Ag@SP at the highest and the lowest concentration tested, respectively, and for Au@SP at both concentrations in a dose-dependent manner. As mentioned before, GM-CSF is a cytokine implicated mainly in cell proliferation and, as a consequence, the SP extract could be able to induce immune cell proliferation that, in combination with a tumor antigen, could help in the activation of the immune system against the tumor cells. Moreover, only Au@SP was able to induce IFN-γ at the highest concentration, while the SP extract induced even a significant decrease on IFN-γ levels compared to the control cells at the lowest concentration tested (Fig. 8). Hence, Au@SP could be the most efficient candidate as an adjuvant for a therapeutic vaccine due to the possibility to induce a more prone Th1 immune response, mediated by IFN-γ and TNF-α, which is desirable for an efficient antitumor immunotherapy. Moreover, the release of the GM-CSF would also aid in the proliferation of the activated immune cells increasing the efficiency of the immunotherapy. Besides, an antibody immune response, mediated by IL-6 and IL-10, could also help in the process of tumor elimination.

The production of immunostimulant and pro-inflammatory cytokines, such as TNF-α, IL-6 and IL-1β by other seaweed like *Ulva intestinalis*, *Sargassum horneri* or *Ulva armoricana*, has already been described [18,102,103]. Besides, AuNPs and AgNPs from chemical synthesis were also able to induce pro-inflammatory cytokines in rodents [104–106]. For that reason, a synergistic effect could be expected on AuNPs and AgNPs synthesized from some seaweed extracts with immunostimulant properties.

The use of metal NPs from green synthesis in the development of new vaccine adjuvants has not been broadly explored so far, although some works have already been published. For instance, the potential adjuvant effect of metal NPs from green synthesis was described for AgNPs obtained from a leaf extract of *Eucalyptus procera* by comparison with alum. These NPs were able to induce a similar immune response to that of this conventional adjuvant in a rabies veterinary vaccine [107]. Likewise, AuNPs synthesized from a glycopolymer containing responsive sugars and catechol functionalities by metal-free reversible addition–fragmentation chain transfer (RAFT), showed good adjuvant properties [108]. The synthetic polymer was able to interact with pathogen recognition receptors (PRR), which are on the surface of innate immune cells. Consequently, the glycoconjugated AuNPs acted as a pathogen-mimetic molecule inducing the activation of these cells.

Oppositely, there are many examples in the bibliography about their use as anti-inflammatory agents, by inhibition of cytokine release. For instance, AgNPs and AuNPs synthesized from an *Asparagus racemosus* root extract [109] or AgNPs European black elderberry fruits extract [110] showed the capacity to modulate cytokine release *in vitro* or *in vivo*, reducing the release of pro-inflammatory cytokines like IL-1β, IL-6, and TNF-α, in inflamed cells.

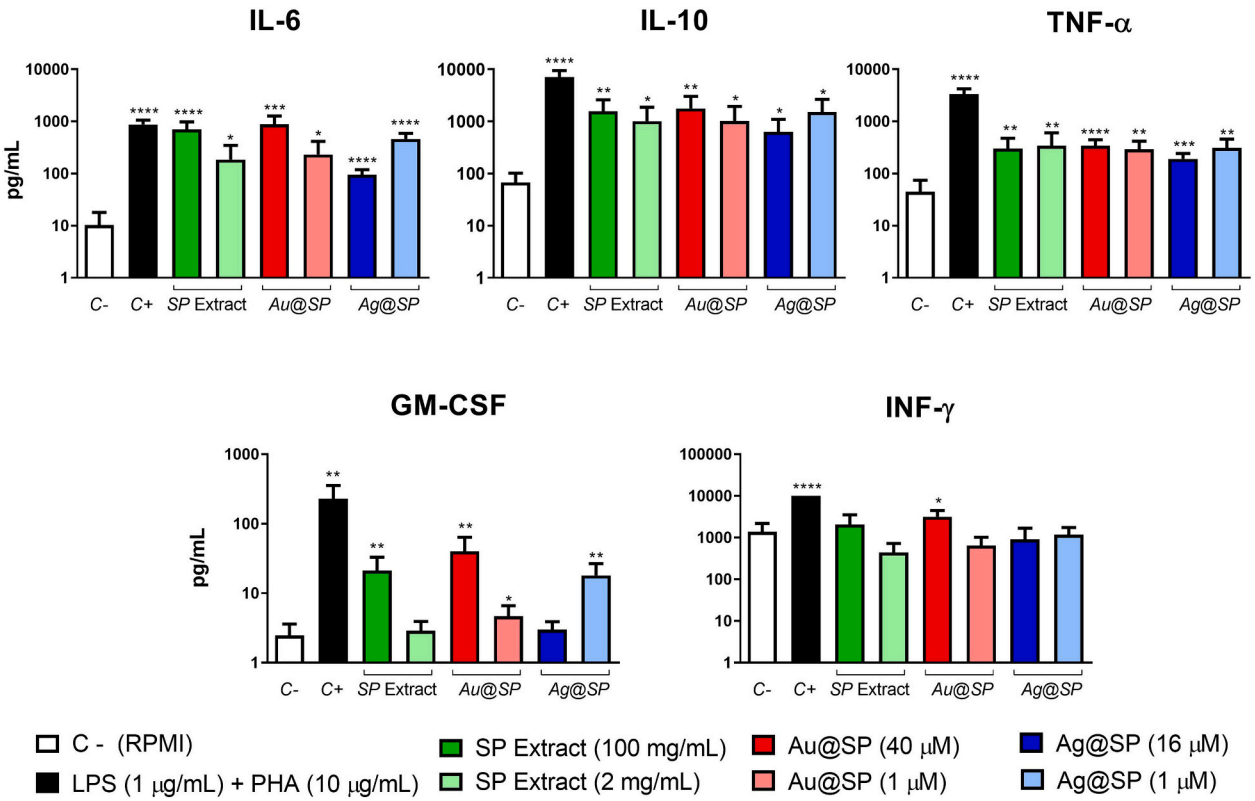

Fig. 8. IL-6, IL-10, TNF-α, GM-CSF and INF-γ production on human peripheral blood mononuclear human cells (hPBMCs) after 24 h of incubation with two different concentrations of the SP extract, Au@SP and Ag@SP. C-: negative control (culture medium). C+: positive control (1 μg/mL LPS + 10 μg/mL PMA). In the graphs: * $P \leq 0.05$, ** $P \leq 0.01$, *** $P \leq 0.001$, **** $P \leq 0.0001$.

From our results, it can be observed that the SP extract possesses stimulatory properties that were preserved in Au@SP and Ag@SP after the nanoparticle synthesis, and even improved in Au@SP with the capacity to induce the release of IFN-γ, a relevant cytokine for a Th1 immune response activation. Moreover, hPBMCs incubated with all the samples showed an increase in the levels of Th2-related cytokines.

Apart from cytokine release, SP extract and Au@SP and Ag@SP were also able to induce ROS release (Fig. 7) and complement activation (Fig. S9), two mechanisms of the innate immune system that were associated with an adjuvant effect and the promotion of a Th1 immune response in a vaccine [111]. For that reason, we believe that Au@SP could be a good adjuvant for a therapeutic or prophylactic vaccine, not only for cancer treatment but also for the treatment of other chronic or infectious diseases.

Among other components, the presence of fucoidans in the extract and the NPs could be responsible for the immunostimulant properties [29,30].

4. Conclusion

The present study has described, for the first time, a successful and rapid synthesis of stabilized AuNPs and AgNPs, in which *Saccorhiza polyschides* is used as a reducing and capping agent. The nanoparticles formed were in the range of 10–20 nm and highly monodisperse. FTIR spectral analysis allowed the identification of different functional groups present in the extract, attributable to different biomolecules such as polysaccharides, proteins and polyphenols, which could be involved in the reduction and in the capping of Au@SP and Ag@SP. The use of SP for the biosynthesis of nanomaterials could expand the range of applications for this species.

Au@SP and Ag@SP showed a dose-dependent antiproliferative effect on a human pulmonary cell line that, in the case of Ag@SP, was superior to the one induced by the SP extract. Interestingly, all the samples induced ROS release at the highest concentration tested; however, an antagonistic effect on ROS release at a low concentration was observed in the presence of a potent ROS inductor, such as PMA. Hence, in contact with certain cells, the samples could induce ROS release and activate different cellular pathways linked to these reactive species. However, in the presence of a powerful ROS inductor, they could have some capacity to neutralize or inhibit high concentrations of these reactive species and, therefore, exert an antioxidant and protective effect on cells due to the fact that very high concentrations of ROS can cause severe damage to cells and even their death.

Besides, the samples were able to induce cytokines implicated in a Th1/Th2 immune response on hPBMc, but only Au@SP produced significant IFN-γ levels. For that reason, Au@SP could be a good adjuvant for a therapeutic or prophylactic vaccine for cancer treatment and prevention.

Ethical conduct

The authors state that they have obtained appropriate institutional review board approval and have followed the principles outlined in the Declaration of Helsinki for all human experimental investigations. In addition, for investigations involving human subjects, informed consent has been obtained from the participants involved.

CRediT authorship contribution statement

NGB: Nanoparticles Methodology, Validation, Formal analysis, Investigation, Data Curation, Writing.

LDG: Biological Methodology, Validation, Formal analysis, Investigation, Data Curation, Writing.

MLV: Conceptualization, Resources, Writing, Supervision.

MG: HPLC Methodology, Validation, Data Curation, Writing.

AC: HPLC Supervision, Validation, Writing.

FB: Conceptualization, Resources, Writing, Supervision.

MCRA: Nanoparticles Conceptualization, Resources, Writing, Supervision, Project administration, Funding acquisition.

RSV: Biological Conceptualization, Resources, Writing, Supervision, Funding acquisition.

Declaration of competing interest

The authors declare that they have no known competing financial interests or personal relationships that could have appeared to influence the work reported in this paper.

Acknowledgements

This research was partially supported by the Xunta de Galicia (Ref.: ED431C 2017/46-GRC and ED431C 2018/54-GRC) and by Project GRC2013-004. LDG acknowledges a fellowship from the Xunta de Galicia (ref. ED481A-2018/294). We would like to thank to Dr. M. Peleteiro for her support in the experiments related to flow cytometry and Luminex technology (Flow Cytometry facilities at the Biomedical Research Center (CINBIO) of the Universidade de Vigo).

Appendix A. Supplementary data

Supplementary data to this article can be found online at https://doi.org/10.1016/j.msec.2021.111960.

References

[1] Azharuddin, M., Zhu G.H., Das D., Ozgur E., Uzun L., Turner A.P.F., Patra H.K.: A repertoire of biomedical applications of noble metal nanoparticles. ChemCom, 6964–6996 (2019).

[2] Anuj, S.A., Gajera H.P., Hirpara D.G., Golakiya B.A.: Bactericidal assessment of nano-silver on emerging and re-emerging human pathogens. J. Trace Elem. Med. Biol. 51, 219–225 (2019).

[3] Sánchez-López, E., Gomes D., Esteruelas G., Bonilla L., Lopez-Machado A.L., Galindo R., Cano A., Espina M., Ettcheto M., Camins A., Silva A.M., Durazzo A., Santini A., Garcia M.L., Souto E.B.: Metal-Based Nanoparticles as Antimicrobial Agents: An Overview. Nanomaterials. 10, 292–335 (2020).

[4] S.M. Amini, Gold nanostructures absorption capacities of various energy forms for thermal therapy applications, J. Therm. Biol. 79 (2019) 81–84.

[5] Bouché, M., Hsu J.C., Dong Y.C., Kim J., Taing K., Cormode D.P.: Recent Advances in Molecular Imaging with Gold Nanoparticles. Bioconjug. Chem. 31, 303–314 (2020).

[6] Falahati, M., Attar F., Sharifi M., Saboury A.A., Salihi A., Aziz F.M., Kostova I., Burda C., Priecel P., Lopez-Sanchez J., Laurent S., Hooshmand N., El-Sayed M.: Gold nanomaterials as key suppliers in biological and chemical sensing, catalysis, and medicine. BBA-General Subjects. 1864, 129435–129462 (2020).

[7] Z.R. Goddard, M.J. Marín, D.A. Russell, M. Searcey, Active targeting of gold nanoparticles as cancer therapeutics, Chem. Soc. Rev. 49 (2020) 8774–8789.

[8] Kang, M.S., Lee S.Y., Kim K.S., Han D.W.: State of the Art Biocompatible Gold Nanoparticles for Cancer Theragnosis. Pharmaceutics. 12, 1–22 (2020).

[9] Kalimuthu, K., Cha B.S., Kim S., Park K.S.: Eco-friendly synthesis and biomedical applications of gold nanoparticles: A review. Microchem. J. 152, 104296–104315 (2020).

[10] A. Rana, K. Yadav, S. Jagadevan, A comprehensive review on green synthesis of nature-inspired metal nanoparticles: mechanism, application and toxicity, J. Clean. Prod. 272 (2020) 122880.

[11] González-Ballesteros, N., Rodríguez-Argüelles, M.C.: Seaweeds: a promising bionanofactory for ecofriendly synthesis of gold and silver nanoparticles. In: Torres, M.D., Kraan, S., Dominguez, H. (eds.) Advances in Green and Sustainable Chemistry. Sustainable Seaweed Tecnologies Cultivation, Biorefinery, and Applications. pp. 507–541.Elsevier, (2020).

[12] R. Chaudhary, K. Nawaz, A. Komal Khan, C.H. Hano, B.H. Abbasi, S. Anjum, An overview of the algae-mediated biosynthesis of nanoparticles and their biomedical applications, Biomolecules. 10 (2020) 1–35.

[13] R. Augustine, A. Hasan, Emerging applications of biocompatible phytosynthesized metal/metal oxide nanoparticles in healthcare, J. Drug Deliv. Sci. Technol. 56 (2020) 101516–101528.

[14] H. Chandra, P. Kumari, E. Bontempi, S. Yadav, Medicinal plants: treasure trove for green synthesis of metallic nanoparticles and their biomedical applications, Biocatal. Agric. Biotechnol. 24 (2020) 101518.

[15] P. Khanna, A. Kaur, D. Goyal, Algae-based metallic nanoparticles: synthesis, characterization and applications, J. Microbiol. Methods 105656-105656 (2019).

[16] Agarwal, H., Nakara A., Shanmugam V.K.: Anti-inflammatory mechanism of various metal and metal oxide nanoparticles synthesized using plant extracts: A review. Biomed. Pharmacother. 109, 2561–2572 (2019).

[17] N. González-Ballesteros, M.C. Rodríguez-Argüelles, S. Prado-López, M. Lastra, M. Grimaldi, A. Cavazza, L. Nasi, G. Salviati, F. Bigi, Macroalgae to nanoparticles: study of *Ulva lactuca* role in biosynthesis of gold and silver nanoparticles and of their cytotoxicity on colon cancer cell lines, Mater. Sci. Eng. C Mater. Biol. Appl. 97 (2019) 498–509.

[18] N. González-Ballesteros, L. Diego-González, M. Lastra-Valdor, M.C. Rodríguez-Argüelles, M. Grimaldi, A. Cavazza, F. Bigi, Simón-Vázquez R.: Immunostimulant and biocompatible gold and silver nanoparticles synthesized by the *Ulva intestinalis* L. aqueous extract, J. Mater. Chem. B 7 (2019) 4677–4691.

[19] N. González-Ballesteros, S. Prado-López, J.B. Rodríguez-González, M. Lastra-Valdor, M.C. Rodríguez-Argüelles, Green synthesis of gold nanoparticles using brown seaweed *Cystoseira baccata*: its activity in colon cancer cells, Colloids Surf. B. Biointerfaces. 153 (2017) 190–198.

[20] M. Silva, F. Gomes, F. Oliveira, S. Morais, Delerue-Matos C.: microwave-assisted alginate extraction from Portuguese *Saccorhiza polyschides* - influence of acid pretreatment, International Journal of Chemical, Molecular, Nuclear, Materials and Metallurgical Engineering. 9 (2015).

[21] Pereira, L.: Seaweed Flora of the European North Atlantic and Mediterranean. In: Kim, S.K. (ed.) Springer Handbook of Marine Biotechnology, pp. 65–178. Springer, (2015).

[22] S.A. Dahoumane, M. Mechouet, K. Wijesekera, C.D.M. Filipe, C. Sicard, D. A. Bazylinski, C. Jeffryes, Algae-mediated biosynthesis of inorganic nanomaterials as a promising route in nanobiotechnology – a review, Green Chem. 19 (2017) 552–587.

[23] K. Oumaskour, N. Boujaber, O. Assobhei, S. Etahiri, Anti-phospholipase A 2 and anti-elastase activity of sixteen marine green and brown algae from the coast of El Jadida-Morocco, Journal of Chemical, Biological and Physical Sciences 6 (2016) 101–108.

[24] M.D. Torres, N. Flórez-Fernández, R. Simón-Vázquez, J.F. Giménez-Abián, J. F. Díaz, Á. González-Fernández, H. Domínguez, Fucoidans: the importance of processing on their anti-tumoral properties, Algal Res. 45 (2020) 1–21.

[25] M. Aquib, M. Asim Farooq, M. Sied Filli, K.O. Boakye-Yiadom, S. Kesse, M. B. Joelle Maviah, R. Mavlyanova, B. Wang, A review on the chemotherapeutic role of fucoidan in cancer as nanomedicine, rjlbpes. 5 (2019).

[26] P. Arumugam, K. Arunkumar, L. Sivakumar, M. Murugan, K. Murugan, Anticancer effect of fucoidan on cell proliferation, cell cycle progression, genetic damage and apoptotic cell death in HepG2 cancer cells, Toxicol. Rep. 6 (2019) 556–563.

[27] Etman, S.M., Elnaggar Y.S.R., Abdallah O.Y.: Fucoidan, a natural biopolymer in cancer combating: From edible algae to nanocarrier tailoring. Int. J. Biol. Macromol. (2020).

[28] van Weelden, G., Bobi M., Okla K., van Weelden W.J., Romano A., Pijnenborg J. M.A.: Fucoidan structure and activity in relation to anti-cancer mechanisms. Marine Drugs. 17, 32–62 (2019).

[29] Ale, M.T., Maruyama H., Tamauchi H., Mikkelsen J.D., Meyer A.S.: Fucoidan from *Sargassum* sp. and *Fucus vesiculosus* reduces cell viability of lung carcinoma and melanoma cells *in vitro* and activates natural killer cells in mice *in vivo*. Int. J. Biol. Macromol. 49, 331–336 (2011).

[30] J. Jin, W. Zhang, J. Du, K. Wong, T. Oda, Q. Yu, Fucoidan can function as an adjuvant in vivo to enhance dendritic cell maturation and function and promote antigen-specific T cell immune responses, PLoS One 9 (2014) e99396.

[31] Hinshaw, D.C., Shevde L.A.: The tumor microenvironment innately modulates cancer progression. Cancer Res. 79, 4557–4566 (2019).

[32] J.M. Pitt, A. Marabelle, A. Eggermont, J. Soria, G. Kroemer, L. Zitvogel, Targeting the tumor microenvironment: removing obstruction to anticancer immune responses and immunotherapy, Ann. Oncol. 27 (2016) 1482–1492.

[33] H. Qian, B. Liu, X. Jiang, Application of nanomaterials in cancer immunotherapy, Materials Today Chemistry. 7 (2018) 53–64.

[34] Y. Yu, C. Hu, L. Xia, J. Wang, Artificial metalloenzyme design with unnatural amino acids and non-native cofactors, ACS Catal. 8 (2018) 1851–1863.

[35] M. Vanneman, G. Dranoff, Combining immunotherapy and targeted therapies in cancer treatment, Nat. Rev. Cancer 12 (2012) 237–251.

[36] Mellman, I., Coukos G., Dranoff G.: Cancer immunotherapy comes of age. Nature. 480, 480–489 (2011).

[37] Galea-Lauri, J., Wells J.W., Darling D., Harrison P., Farzaneh F.: strategies for antigen choice and priming of dendritic cells influence the polarization and efficacy of antitumor T-cell responses in dendritic cell-based cancer vaccination. Cancer Immunol. Immunother. 53, 963–977 (2004).

[38] K. Vermaelen, Vaccine strategies to improve anti-cancer cellular immune responses, Front. Immunol. 10 (2019).

[39] R. Simón-Vázquez, M. Peleteiro, A. González-Fernandez, Polymeric nanostructure vaccines: applications and challenges, Expert Opin Drug Deliv. 17 (2020) 1007–1023.

[40] M. Carocho, I.C.F.R. Ferreira, The role of phenolic compounds in the fight against cancer – a review, Anti Cancer Agents Med. Chem. 13 (2013) 1236–1258.

[41] de la Rosa, L. A., Moreno-Escamilla, J.O., Rodrigo-García, J., Alvarez-Parrilla, E.: Chapter 12 - phenolic compounds. In: Anonymous Postharvest Physiology and Biochemistry of Fruits and Vegetables, pp. 253–271. (2019).

[42] N. González-Ballesteros, J.B. Rodríguez-González, M. Lastra-Valdor, M. C. Rodríguez-Argüelles, New application of two Antarctic macroalgae *Palmaria decipiens* and *Desmarestia menziesii* in the synthesis of gold and silver nanoparticles, Polar Sci. 15 (2018) 49–54.

[43] Tiloke, C., Phulukdaree A., Anand K., Gengan R.M., Chuturgoon A.A.: *Moringa oleifera* Gold Nanoparticles Modulate Oncogenes, Tumor Suppressor Genes, and Caspase-9 Splice Variants in A549 Cells. J. Cell. Biochem. 117, 2302–2314 (2016).

[44] Porcaro, F., Battocchio C., Antoccia A., Fratoddi I., Venditti I., Fracassi A., Luisetto I., Russo M.V., Polzonetti G.: Synthesis of functionalized gold nanoparticles capped with 3-mercapto-1-propansulfonate and 1-thioglucose mixed thiols and "*in vitro*" bioresponse. Colloids Surf. B. Biointerfaces. 142, 408–416 (2016).

[45] S. Bhattacharjee, DLS and zeta potential – what they are and what they are not? J. Control. Release 235 (2016) 337–351.

[46] Rodrigues, D., Freitas A.C., Pereira L., Rocha-Santos T.A.P., Vasconcelos M.W., Roriz M., Rodríguez-Alcalá L.M., Gomes A.M.P., Duarte A.C.: Chemical composition of red, brown and green macroalgae from Buarcos bay in Central West Coast of Portugal. Food Chem. 183, 197–207 (2015).

[47] N. Kolb, L. Vallorani, N. Milanovi, V. Stocchi, Evaluation of marine algae Wakame (*Undaria pinnatifida*) and Kombu (*Laminaria digitata japonica*) as food supplements, Food Technol. Biotechnol. 42 (2004) 57–61.

[48] E.M. Balboa, C. Gallego-Fabrega, A. Moure, H. Dominguez, Study of the seasonal variation on proximate composition of oven-dried *Sargassum muticum* biomass collected in Vigo Ria, Spain, J. Appl. Phycol. 28 (2016) 1943–1953.

[49] J.S. Garcia, V. Palacios, A. Roldán, Nutritional potential of four seaweed species collected in the barbate estuary (Gulf of Cadiz, Spain), J. Nutr. Food Sci. 06 (2016).

[50] G. Jard, H. Marfaing, H. Carrère, J.P. Delgenes, J.P. Steyer, C. Dumas, French Brittany macroalgae screening: composition and methane potential for potential alternative sources of energy and products, Bioresour. Technol. 144 (2013) 492–498.

[51] B.A. Macler, Regulation of carbon flow by nitrogen and light in the red alga, *Gelidium coulteri*, Plant Physiol. 82 (1986) 136–141.

[52] E. Gómez-Ordóñez, A. Jiménez-Escrig, P. Rupérez, Dietary fibre and physicochemical properties of several edible seaweeds from the northwestern Spanish coast, Food Res. Int. 43 (2010) 2289–2294.

[53] L. Pereira, A. Sousa, H. Coelho, A.M. Amado, P.J.A. Ribeiro-Claro, Use of FTIR, FT-Raman and 13C-NMR spectroscopy for identification of some seaweed phycocolloids, Biomol. Eng. 20 (2003) 223–228.

[54] D.I. Sánchez-Machado, J. López-Cervantes, J. López-Hernández, P. Paseiro-Losada, J. Simal-Lozano, Determination of the uronic acid composition of seaweed dietary fibre by HPLC, Biomed. Chromatogr. 18 (2004) 90–97.

[55] Lee, D.S., Lee C.K., Jang Y.S.: Dietary fiber content of seaweeds in Korea. Bulletin of the National Fishery Research and Development Agency Korea. 52, 99–106 (1996).

[56] Wang, D., Markus J., Wang C., Kim Y.J., Mathiyalagan R., Aceituno-Castro V., Ahn S., Yang D.C.: Green synthesis of gold and silver nanoparticles using aqueous extract of *Cibotium barometz* root. Artif. Cells Nanomed. Biotechnol. 45, 1548–1555 (2017).

[57] Pereira, L., Gheda S.F., Ribeiro-Claro P.J.A.: Analysis by vibrational spectroscopy of seaweed polysaccharides with potential use in food, pharmaceutical, and cosmetic industries. 2013 (2013).

[58] Riazia, M., Keshtkarb A.R., Moosaviana M.A.: Biosorption of Th(IV) in a fixed-bed column by Ca-pretreated *Cystoseira indica*. 4, 1890–1898 (2016).

[59] H.S.A. Koh, J. Lu, W. Zhou, Structure characterization and antioxidant activity of fucoidan isolated from *Undaria pinnatifida* grown in New Zealand, Carbohydr. Polym. 212 (2019) 178–185.

[60] P. Lodeiro, J.L. Barriada, R. Herrero, M.E. Sastre de Vicente, The marine macroalga *Cystoseira baccata* as biosorbent for cadmium(II) and lead(II) removal: kinetic and equilibrium studies, Environ. Pollut. 142 (2006) 264–273.

[61] T. Stalin Dhas, V. Ganesh Kumar, L. Stanley Abraham, V. Karthick, K. Govindaraju, *Sargassum myriocystum* mediated biosynthesis of gold nanoparticles, Spectrochim. Acta A Mol. Biomol. Spectrosc. 99 (2012) 97–101.

[62] S. Pinteus, J. Silva, C. Alves, A. Horta, N. Fino, A.I. Rodrigues, S. Mendes, R. Pedrosa, Cytoprotective effect of seaweeds with high antioxidant activity from the Peniche coast (Portugal), Food Chem. 218 (2017) 591–599.

[63] N. González-Ballesteros, M.C. Rodríguez-Argüelles, M. Lastra-Valdor, G. González-Mediero, S. Rey-Cao, M. Grimaldi, A. Cavazza, F. Bigi, Synthesis of silver and gold nanoparticles by *Sargassum muticum* biomolecules and evaluation of their antioxidant activity and antibacterial properties, J Nanostructure Chem. 10 (2020) 317–330.

[64] Palanisamy, S., Rajasekar P., Vijayaprasath G., Ravi G., Manikandan R., Prabhu N.M.: A green route to synthesis silver nanoparticles using *Sargassum polycystum* and its antioxidant and cytotoxic effects: An *in vitro* analysis. Mater. Lett. 189, 196–200 (2017).

[65] Muthukumar, H., Palanirajan S.K., Shanmugam M.K., Gummadi S.N.: Plant extract mediated synthesis enhanced the functional properties of silver ferrite nanoparticles over chemical mediated synthesis. Biotechnology Reports. 26, 1–10 (2020).

[66] Cyril, N., George J.B., Joseph L., Raghavamenon A.C., Sylas V.P.: Assessment of antioxidant, antibacterial and antiproliferative (lung cancer cell line A549) activities of green synthesized silver nanoparticles from *Derris trifoliata*. Toxicol Res. 8, 297–308 (2019).

[67] Soshnikova, V., Kim Y.J., Singh P., Huo Y., Markus J., Ahn S., Castro-Aceituno V., Kang J., Chokkalingam M., Mathiyalagan R., Yang D.C.: Cardamom fruits as a green resource for facile synthesis of gold and silver nanoparticles and their biological applications. Artif. Cells Nanomed. Biotechnol. 46, 108–117 (2018).

[68] G. Bonaventura, V. La Cognata, R. Iemmolo, M. Zimbone, A. Contino, G. Maccarrone, B. Failla, M.L. Barcellona, F.L. Conforti, V. D'Agata, S. Cavallaro, Ag-NPs induce apoptosis, mitochondrial damages and MT3/OSGIN2 expression changes in an *in vitro* model of human dental-pulp-stem-cells-derived neurons, Neurotoxicology. 67 (2018) 84–93.

[69] A. Barbasz, M. Oćwieja, M. Roman, Toxicity of silver nanoparticles towards tumoral human cell lines U-937 and HL-60, Colloids Surf. B. Biointerfaces. 156 (2017) 397–404.

[70] P. Singh, S. Pandit, V.R.S.S. Mokkapati, A. Garg, V. Ravikumar, I. Mijakovic, Gold nanoparticles in diagnostics and therapeutics for human cancer, Int. J. Mol. Sci. 19 (2018) 1979–1995.

[72] P. Chairuangkitti, S. Lawanprasert, S. Roytrakul, S. Aueviriyavit, D. Phummiratch, K. Kulthong, P. Chanvorachote, R. Maniratanachote, Silver nanoparticles induce toxicity in A549 cells via ROS-dependent and ROS-independent pathways, Toxicol. in Vitro 27 (2013) 330–338.

[73] Mateo, D., Morales P., Ávalos A., Haza A.I.: Oxidative stress contributes to gold nanoparticle-induced cytotoxicity in human tumor cells. Toxicol. Mech. Methods 24, 161–172 (2014).

[81] S. Gurunathan, J.K. Jeong, J.W. Han, X.F. Zhang, J.H. Park, J.H. Kim, Multidimensional effects of biologically synthesized silver nanoparticles in *Helicobacter pylori*, *Helicobacter felis*, and human lung (L132) and lung carcinoma A549 cells, Nanoscale Res. Lett. 10 (2015).

[82] S.P. Vinay, Udayabhanu, G. Nagaraju, C.P. Chandrappa, N. Chandrasekhar, A novel, green, rapid, nonchemical route hydrothermal assisted biosynthesis of Ag nanomaterial by blushwood berry extract and evaluation of its diverse applications, Appl. Nanosci. 10 (2020) 3341–3351.

[83] Foldbjerg, R., Dang D.A., Autrup H.: Cytotoxicity and genotoxicity of silver nanoparticles in the human lung cancer cell line, A549. Arch. Toxicol. 85, 743–750 (2011).

[84] Lee, Y.S., Kim D.W., Lee Y.H., Oh J.H., Yoon S., Choi M.S., Lee S.K., Kim J.W., Lee K., Song C.W.: Silver nanoparticles induce apoptosis and G2/M arrest via PKCζ-dependent signaling in A549 lung cells. Arch. Toxicol. 85, 1529–1540 (2011).

[85] El Badawy, A.M., Silva R.G., Morris B., Scheckel K.G., Suidan M.T., Tolaymat T. M.: Surface Charge-Dependent Toxicity of Silver Nanoparticles. Environ Sci Technol. 45, 283–287 (2011).

[86] C. Beer, R. Foldbjerg, Y. Hayashi, D.S. Sutherland, H. Autrup, Toxicity of silver nanoparticles—nanoparticle or silver ion, Toxicol. Lett. 208 (2012) 286–292.

[87] B. Sun, N. Hu, L. Han, Y. Pi, Y. Gao, K. Chen, Anticancer activity of green synthesised gold nanoparticles from *Marsdenia tenacissima* inhibits A549 cell proliferation through the apoptotic pathway, Artif. Cells Nanomed. Biotechnol. 47 (2019) 4012–4019.

[88] Anantharaju, P.G., Gowda P.C., Vimalambike M.G., Madhunapantula S.V.: An overview on the role of dietary phenolics for the treatment of cancers. Nutr. J. 15, 1–16 (2016).

[89] Mortimer, G.M., Minchin, R.F.: Nanotoxicology and nanovaccines. In: Skwarczynski, M., Toth, I. (eds.) Micro- and Nanotechnology in Vaccine Development, pp. 373–392.William Andrew Publishing, Oxford (2017).

[90] Y. Shang, L. Tian, T. Chen, X. Liu, J. Zhang, D. Liu, J. Wei, W. Fang, Y. Chen, D. Shang, CXCL1 promotes the proliferation of neural stem cells by stimulating the generation of reactive oxygen species in APP/PS1 mice, Biochem. Biophys. Res. Commun. 515 (2019) 201–206.

[91] F. Kotsias, E. Hoffmann, S. Amigorena, A. Savina, Reactive oxygen species production in the phagosome: impact on antigen presentation in dendritic cells, Antioxid. Redox Signal. 18 (2013) 714–729.

[92] Beer, C.: Nanotoxicology and regulatory affairs. In: Howard, K.A., Vorup-Jensen, T., Peer, D. (eds.) Nanomedicine. Advances in Delivery Science and Technology, pp. 279–310.Springer, New York (2016).

[93] Tan, H.Y., Wang N., Li S., Hong M., Wang X., Feng Y.: The reactive oxygen species in macrophage polarization: reflecting its dual role in progression and treatment of human diseases. Oxidative Med. Cell. Longev. Volume 2016, 1–16 (2016).

[94] L. Virág, R.I. Jaén, Z. Regdon, L. Boscá, P. Prieto, Self-defense of macrophages against oxidative injury: fighting for their own survival, Redox Biol. 26 (2019) 1–9.

[95] M.D. Ferrer, A. Sureda, A. Mestre, J.A. Tur, A. Pons, The double edge of reactive oxygen species as damaging and signaling molecules in HL60 cell culture, Cell. Physiol. Biochem. 25 (2010) 241–252.

[96] A. Barbasz, M. Oćwieja, S. Walas, Toxicological effects of three types of silver nanoparticles and their salt precursors acting on human U-937 and HL-60 cells, Toxicol. Mech. Methods 27 (2017) 58–71.

[97] A. Avalos, A.I. Haza, D. Mateo, P. Morales, Cytotoxicity and ROS production of manufactured silver nanoparticles of different sizes in hepatoma and leukemia cells, J. Appl. Toxicol. 34 (2014) 413–423.

[98] S. Patil, R. Chandrasekaran, Biogenic nanoparticles: a comprehensive perspective in synthesis, characterization, application and its challenges, J. Genet. Eng. Biotechnol. 18 (2020) 1–23.

[99] O'Shea, J.J., Gadina, M., Siegel, R.M.: Cytokines and cytokine receptors. In: Rich, R.R., Fleisher, T.A., Shearer, W.T., Schroeder, H.W., Frew, A.J., Weyand, C.M. (eds.) Clinical Immunology. Principles and Practice, pp. 127–155.Elsevier, (2019).

[100] Muñoz-Carrillo, J.L., Contreras Cordero, J.F., Gutiérrez-Coronado, O., Villalobos-Gutiérrez, P.T., Ramos-Gracia, L.G., Hernández-Reyes, V.E.: Cytokine profiling plays a crucial role in activating immune system to clear infectious pathogens. In: Tyagi, R.K., Bisen, P.S. (eds.) Immune Response Activation and Inmunostimulation, pp. 1–30.IntechOpen, (2018).

[101] J. O'shea, C.M. Tato, R. Siegel, Cytokines and cytokine receptors, in: Anonymous Clinical Immunology, 2008, pp. 139–171.

[102] M. Berri, M. Olivier, S. Holbert, J. Dupont, H. Demais, M. Le Goff, P.N. Collen, Ulvan from *Ulva armoricana* (Chlorophyta) activates the PI3K/Akt signalling

pathway via TLR4 to induce intestinal cytokine production, Algal Res. 28 (2017) 39–47.
[103] Herath, K.H.I.N.M., Cho J., Kim A., Kim H., Kim H., E.J., Kim H.J., Kim M.S., Ahn G., Jeon Y., Jee Y.: Differential modulation of immune response and cytokine profiles of Sargassum horneri ethanol extract in murine spleen with or without Concanavalin a stimulation. Biomed. Pharmacother. 110, 930–942 (2019).
[104] Al-Harbi, N., Alrashood S.T., Siddiqi N.J., Arafah M.M., Ekhzaimy A., Khan H.A.: Effect of naked and PEG-coated gold nanoparticles on histopathology and cytokines expression in rat liver and kidneys. Nanomedicine. 15, 289–302 (2019).
[105] H.A. Khan, K.E. Ibrahim, S.T. Alrashood, S. Alamery, S.H. Alrokayan, N. Al-Harbi, M. Al-Mutary, S.H. Sobki, I. Khan, Immunohistochemistry of IL-1β, IL-6 and TNF-α in spleens of mice treated with gold nanoparticles, Saudi Journal of Biological Sciences. 27 (2020) 1163–1168.
[106] Huang, C., Hsiao I., Lin H., Wang C., Huang Y., Chuang C.: Silver nanoparticles affect on gene expression of inflammatory and neurodegenerative responses in mouse brain neural cells. Environ. Res. 136, 253–263 (2015).
[107] Asgary, V., Shoari A., Baghbani-Arani F., Sadat Shandiz S.A., Khosravy M.S., Janani A., Bigdeli R., Bashar R., Cohan R.A.: Green synthesis and evaluation of silver nanoparticles as adjuvant in rabies veterinary vaccine. Int. J. Nanomedicine 11, 3597–3605 (2016).
[108] Wen, M., Liu M., Xue W., Yang K., Chen G., Zhang W.: Simple and Green Strategy for the Synthesis of "Pathogen-Mimetic" Glycoadjuvant@AuNPs by Combination of Photoinduced RAFT and Bioinspired Dopamine Chemistry. ACS Macro Lett. 7, 70–74 (2018).
[109] Amina, M., Al Musayeib N.M., Alarfaj N.A., El-Tohamy M.F., Al-Hamoud G.A.: Antibacterial and Immunomodulatory Potentials of Biosynthesized Ag, Au, Ag-Au Bimetallic Alloy Nanoparticles Using the *Asparagus racemosus* Root Extract. Nanomaterials. 10, 1–20 (2020).
[110] David, L., Moldovan B., Vulcu A., Olenic L., Perde-Schrepler M., Fischer-Fodor E., Florea A., Crisan M., Chiorean I., Clichici S., Filip G.A.: Green synthesis, characterization and anti-inflammatory activity of silver nanoparticles using European black elderberry fruits extract. Colloids Surf. B. Biointerfaces. 122, 767–777 (2014).
[111] Siegrist, C.A.: 2 - Vaccine immunology. In: Plotkin, S.A., Orenstein, W.A., Offit, P. A., Edwards, K.M. (eds.) Plotkin's Vaccines, pp. 16–34.Elsevier, (2018).